Vol. 388: 121–135, 2009
doi: 10.3354/meps08167

MARINE ECOLOGY PROGRESS SERIES
Mar Ecol Prog Ser

Published August 19

Colonisation and connectivity by intertidal limpets among New Zealand, Chatham and Sub-Antarctic Islands. II. Oceanographic connections

Stephen M. Chiswell*

National Institute of Water and Atmospheric Research, PO Box 14-901, Wellington, New Zealand

ABSTRACT: Satellite-derived measurements of ocean currents made since 1993 were used to examine whether present-day oceanic circulation can explain 2 observed genetic lineages of the intertidal limpet *Cellana strigilis* in the New Zealand region. The western lineage comprises the South Island of New Zealand, Auckland and Campbell Islands, and the eastern lineage comprises the Chatham, Antipodes and Bounty Islands. Satellite-derived currents were used to simulate potential larval trajectories and hence estimate dispersal times between the islands. A random walk was added to the model to account for missing high-frequency variance in the satellite-derived currents. Surface drifters were used to calibrate the model. Minimum simulated dispersal times between the islands can easily explain the separation of the 2 lineages, but are too long, except between Antipodes and Bounty Islands, to explain the observed homogeneity within the lineages. It is suggested that rare long-distance dispersal events in the ocean, occurring too infrequently to be observed in 15 yr of simulations, influence the gene flow, and the frequency of these events may be estimated by fitting analytical functions to histograms of simulated larval dispersal. For some island pairs that are genetically connected, the maximum 10 d larval duration of *C. strigilis* appears at the 10^{-4} percentile. If this genetic connection occurs via larval dispersal, this suggests that connection may occur even when fewer than 1 in 1 million dispersal times is shorter than the larval duration.

KEY WORDS: *Cellana* · Connectivity · Modelling · Larval connections · Dispersal time

INTRODUCTION

Many sub-tidal and intertidal organisms have a planktonic larval phase that results in oceanic dispersal. The duration of this pelagic larval phase can vary from hours to months. For example, New Zealand abalone *Haliotis iris* have a larval lifetime of up to 10 d (Stephens et al. 2006 and references therein), New Zealand sea urchins *Evechinus chloroticus* have a larval lifetime of 30 to 60 d (Walker 1984), and New Zealand rock lobsters *Jasus edwardsii* have a larval lifetime of between 12 and 24 mo (Booth 2002). *Cellana strigilis* limpets are thought to have a 3 to 10 d larval phase (Creese 1981).

If long-distance dispersal of larvae via ocean currents is the predominant means of gene flow between islands, one might expect genetic distributions of different island populations to reflect the dispersal times between the islands: populations that are connected by dispersal times <1 larval lifetime might be expected to show less genetic difference than those separated by dispersal times >1 larval lifetime.

Goldstien et al. (2009, this volume) showed that 2 genetic lineages of the *Cellana strigilis* complex exist in the New Zealand region. The western lineage comprises the South Island (including Stewart Island) of New Zealand together with Auckland and Campbell Islands, and the eastern lineage comprises the Chatham, Antipodes and Bounty Islands (Fig. 1). Phylogenetic relationships suggest that the 2 lineages diverged 2 to 5 million yr ago (Ma). There was no observed genetic variation within each lineage, thus the data suggest not only a lack of present-day connection between the 2 lineages, but that there is present-day

*Email: s.chiswell@niwa.cri.nz

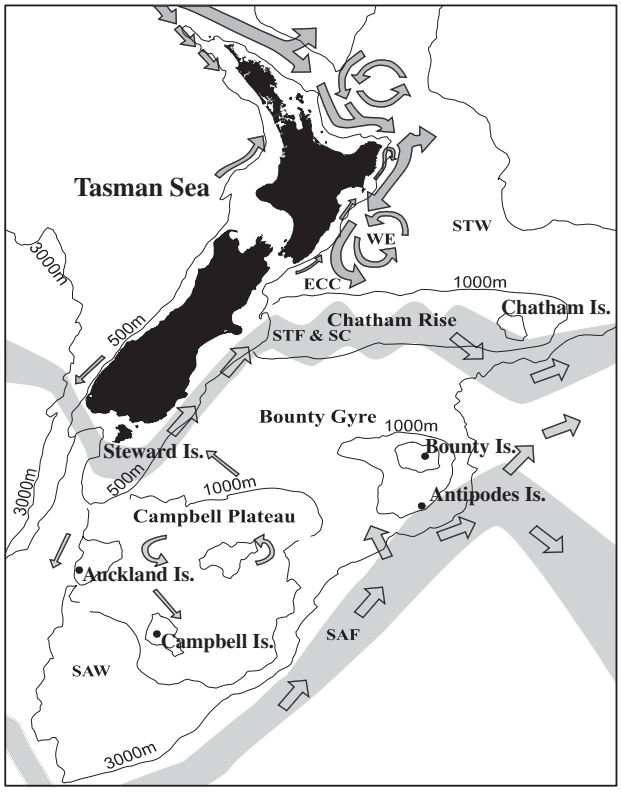

Fig. 1. Bathymetry and schematic surface circulation in the New Zealand region. The Subtropical Front (STF) and Sub-Antarctic Front (SAF) are shown in grey

connection within each lineage. If present-day connections via larval dispersal do not exist, then alternative explanations must be found to account for the observed genetic homogeneity.

This article has 2 aims. One is to estimate present-day larval dispersal times between the islands in the New Zealand region. The second is to determine whether the observed *Cellana strigilis* genetics can be explained by these dispersal times. The region of interest encompasses the main islands of New Zealand (North, South and Stewart Islands), which are assumed to represent 1 genetic stock. The offshore islands are Auckland, Campbell, Antipodes, Bounty and Chatham Islands (Fig. 1). This work is motivated by the desire to explain the *Cellana* genetics but is kept general enough so that the results are applicable to other species, thus the North Island is included even though *C. strigilis* does not occur there.

A large body of literature has been devoted to the question of just how much gene flow between populations is required to maintain genetic homogeneity (e.g. Futuyma 1998), and while the answers presumably depend on relative population sizes and the presence of natural selection processes, they tend towards 'not much' rather than 'a lot' – for example, the '1-migrant-per-generation' rule (Mills & Allendorf 1966, Mace & Lande 1991) indicates very infrequent connection may be sufficient to maintain genetic homogeneity. Certainly a lot less larval transport between 2 locations is required to maintain genetic homogeneity than is required to maintain ecological connectivity, where ecological connectivity suggests a direct link between the dynamics of individual populations (Cowen et al. 2000, Cowen & Sponaugle 2009). Thus, it is likely that genetic homogeneity could be maintained by highly infrequent episodic events or 'rare long-distance dispersal events' (e.g. Kinlan et al. 2005).

Satellite-derived currents can be used with Lagrangian particle tracking methods (see 'Materials and methods; Larval tracking' for more detail) to seed numerical oceans with numerical larvae and follow their trajectories. In principle, one could use such methods to run larval tracking simulations, taking hatching locations, rates and mortality into account, to model the gene flow between islands. If one knew the required gene flow to maintain connectivity, one could determine whether larval dispersal were maintaining the genetics, or whether some other explanation such as rafting was needed. Alternatively, one could assume larval dispersal is responsible for the genetics and back-calculate estimates of the gene flow requirements. However, as is shown later, with only 15 yr of satellite observations and low arrival rates at destination islands (most larvae simply are lost at sea), it is very difficult to obtain sufficient numerical larvae to arrive at any islands in order to make estimates of the long-term gene flow.

Instead, this article takes a slightly different approach. The ocean is seeded with as many numerical larvae as is practicable, and the frequency histograms of dispersal times are accumulated for each island pair (source and destination island). In the best case, there were approximately 4000 simulated arrivals, but for most island pairs there were considerably fewer arrivals; in the worst case, there were only 5 arrivals. To estimate the statistics of the observed distributions, a fit is made using log-normal distribution, and the dispersal time statistics (i.e. mean and various percentiles) are estimated from the analytic fit. Under the assumption that viable gene flow can only occur when dispersal times are less than the maximum larval duration for *Cellana* spp. (10 d), the corresponding percentile values for this maximum larval duration are calculated. These percentiles turn out to be surprisingly low even for island pairs that are observed to have no genetic variation. This suggests that if gene flow between these islands is due to larval dispersal, then it is due to extremely rare events.

Mortality was not included in the simulations because the main aim of this work was to compute dis-

persal times that can then be interpreted according to the species of interest. In addition, mortality is difficult to estimate, probably different for different species, and likely to be highly variable even within 1 species. However, mortality does affect the age distributions of larvae arriving at a destination island, because older larvae will suffer more mortality than younger larvae. Thus, mortality must be taken into account if one's interest is the age of settling larvae, in which case one can multiply the frequency distribution of dispersal times by the age-dependent survival rate of larvae.

Satellite-altimeter derived surface currents are available from the US-French Topex/Poseidon satellite and its successors in gridded form as the AVISO dataset (CNES France). However, AVISO data are not without limitations. AVISO currents are anomalies about a mean surface velocity field, which must be determined independently. Here the mean field is derived from satellite-tracked 'holey-sock' drifters that have been deployed for many years as part of the Global Drifter Program (GDP; e.g. Hansen & Poulain 1996). In addition, Chiswell & Rickard (2008) suggested that the AVISO currents are missing high-frequency mesoscale eddy variability, so that diffusion caused by this variability may be underestimated. Here, a random-walk term was added to the larval tracking model to account for this missing diffusion, and the GDP data provide a means to calibrate the random walk term.

This article proceeds as follows. First, a general description of the circulation around New Zealand is given. The Materials and Methods section describes the GDP data and the model along with details of how the model was calibrated. Computed dispersal distances are then shown as a function of time to illustrate the lack of seasonality in the results. The dispersal times and their histograms are then presented, and finally, the Discussion summarises the main conclusions and gives some biological interpretation.

MATERIALS AND METHODS

Circulation around New Zealand. New Zealand sits in the predominantly eastward flowing southern arm of the South Pacific gyre. To the north, the Tasman Front flows across the Tasman Sea at about 34° S (Fig. 1). This flow then attaches to the east coast of the North Island as the East Auckland and East Cape Currents. The East Cape Current recirculates around the Wairarapa Eddy and then flows eastward along the northern flank of the Chatham Rise. The Subtropical Front flows across the Tasman Sea at about 45° S, and then flows north-east along the east coast of the South Island, where it is known locally as the Southland Front or Southland Current. The front peels away from the coast to flow eastwards along the Chatham Rise. At the eastern end of the rise, the Subtropical Front dips to the south-east. To the south of the region, the Antarctic Circumpolar Current flows strongly along the flanks of the Campbell Plateau in a general easterly direction.

Global Drifter Program drifters. Global Drifter Program (GDP) drifters are drogued at a nominal 15 m depth and transmit their position by satellite. Quality controlled and 6-hourly interpolated GDP data are available from Marine Environmental Data Services (www.meds-sdmm.dfo-mpo.gc.ca). The nominal 15 m depth of the drogues is well within the mixed-layer in the New Zealand region, and the drogues can be regarded as reasonable followers of water parcels in the mixed layer. To the extent that larvae drift passively and remain in the mixed layer, the GDP drogue trajectories are expected to be accurate indicators of potential larval trajectories.

There is some suggestion that holey-sock drifters are influenced by the wind (Niiler et al. 1995), and that if the winds are known accurately enough, this wind-slippage can be corrected. In principle, one could use hindcast winds to correct the GDP drifter velocities for slippage, but it was felt that these wind data are not accurate enough, nor is the drifter response to the wind known well enough, to warrant such a correction.

Fig. 2 shows the tracks of GDP drifters passing through the New Zealand region between 1979 and

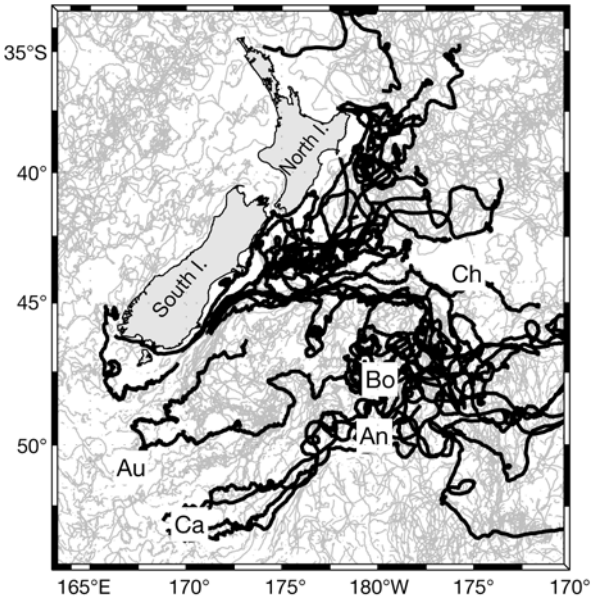

Fig. 2. Global Drifter Program (GDP) drifter tracks in New Zealand region. Those passing within 30 km of islands are shown in black. Au: Auckland, Ca: Campbell, Bo: Bounty, An: Antipodes, Ch: Chatham Islands

2007. While no drifters were released from the islands considered here, a few passed close enough to some islands that they represent potential larval tracks from those islands. If, somewhat arbitrarily, 'close enough' is defined to be 30 km, then 21 drifter trajectories passed close to mainland New Zealand, and 16 passed close to the offshore islands.

AVISO. AVISO Maps of Sea Level Anomaly (MSLA) made available by AVISO/Altimetry, Space Oceanography Division France provide time-varying sea level determined from merged TOPEX/Poseidon, European Remote Sensing (ERS-1) satellites and their successors. Surface zonal and meridional currents were computed from these sea level fields assuming geostrophy (e.g. Pond & Pickard 1978). The TOPEX/Poseidon satellite was launched in October 1992, and data were available for the present study from January 1993 to mid-2008.

Altimeter data are generally considered to be variations about the mean field, which must be determined independently. The mean surface velocity field (Fig. 3) used here was derived from the GDP drifter data shown in Fig. 2. The GDP drifter data were binned into 2° latitude and longitude bins, and the mean velocity within that bin was assigned to the centre of the bin. Bins were overlapped to provide a mean field with 1° resolution as detailed by Chiswell & Rickard (2006). This mean field and AVISO velocities were interpolated onto a 1/12° grid for the simulations.

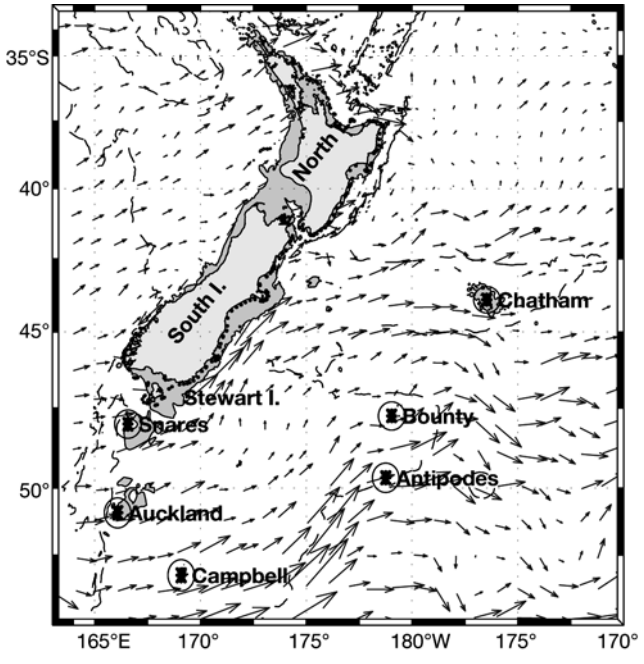

Fig. 3. Mean surface velocity field derived from the Global Drifter Program (GDP) drifters (grey vectors). The GDP drifter data were binned into 2° latitude and longitude bins, and the mean velocity within a bin was assigned to the centre of the bin. Dots show larval release locations. Around the main islands of New Zealand (North, South, Stewart), release locations were approximately 16 km apart, and 20 km from the coast. Around the offshore islands (Auckland, Campbell, Antipodes, Bounty and Chatham), release locations were in a grid centred on the island. Depths less than 125 m are shaded, and the 2000 m isobath is shown. Circles around the islands indicate a 50 km arrival distance (see 'Dispersal times')

Larval tracking. Larval trajectories can be simulated from the AVISO currents by numerically seeding the ocean with 'larvae' at specified hatching locations and using standard particle-following Lagrangian techniques. Trajectories computed from AVISO currents show less dispersal than expected in reality because of a loss of relatively high-frequency energy (Chiswell & Rickard 2008). To compensate for this lack of dispersal, a Markov 0 random-walk diffusion term (e.g. Rupolo 2007) was added to the larval displacement at each time step. Similar methods are often used to parameterise sub-grid scale diffusion (for examples, see Olson 2007). The zonal displacement, x, at time $t + \Delta_t$ is thus:

$$x_{t+\Delta_t} = L(x_t, u_{t,t+\Delta_t}) + \sqrt{2K^+\Delta_t}\,\Re_{0,1} \quad (1)$$

where u_t is velocity at time t, and L is a fourth-order Runge-Kutta Lagrangian integrator, K^+ is the added eddy diffusivity and $\Re_{0,1}$ is a random number drawn from a Gaussian distribution having mean = 0 and SD = 1. The choice of eddy diffusivity, K^+, for the added dispersal can be made by comparing the modelled dispersal from individual islands to the observed dispersal of the GDP drifters that passed close to each island, as discussed in the next section.

The hatching locations were approximately uniformly distributed about 16 km apart around the main islands of New Zealand (Snares Island is considered here as part of mainland New Zealand because it is so close to the South Island) and in a grid centred on each offshore island (Fig. 3). Hatching was assumed to take place about 7 km off the coast for the main islands of New Zealand because AVISO lacks details on the coastal circulation. This offshore transport is driven by winds and coastal processes not included in our model. Twenty-five larvae were released at each offshore island spread over a grid as shown in Fig. 3.

By repeatedly seeding each hatching location at some time interval, in this case every 25 d over 15 yr from 1 January 1993 to 18 May 2007 (i.e. a total of 211 simulations), and computing each trajectory for 300 d, one can build up a set of trajectories from each hatching location. The 25 d interval between simulations is comparable to the Eulerian timescale in the region (Chiswell et al. 2007), so that each trajectory will be statistically independent. When collapsed to the same time origin, the different trajectories are assumed to statistically represent the probability of potential larval dispersal. For example, the likely dispersal at 10 d from any hatching

site can be estimated from the ensemble of simulated positions 10 d after release from that location.

By necessity, the 15 yr of AVISO-derived currents used in the simulations data are assumed to be representative of the long-term oceanographic conditions in the region, but one can test for both seasonal and inter-annual trends in the modelled dispersal (see 'Dispersal times').

The currents modelled here are surface currents, and are likely to be only representative of currents in the mixed layer. The model larvae act as passive surface tracers, i.e. they reside in the surface layers and have no directed swimming ability. Real larvae that show significant vertical migration will experience deeper, slower currents and so may show less dispersal than calculated here.

Model calibration. Calibration of the added eddy diffusivity, K^+, can be made by running the model with several values of K^+, and comparing the overall eddy diffusivity in the modelled larvae to both previous estimates of eddy diffusivity and to eddy diffusivity calculated directly from the GDP drifters in the region. Chiswell (unpubl. data) made estimates of surface eddy diffusivity in the South Pacific Ocean from 2 different methods. There is some difference between the 2 methods for the region east of New Zealand, but eddy diffusivity was found to be anisotropic, and values were 5 to 10×10^3 m^2 s^{-1} and 2 to 4×10^3 m^2 s^{-1} for the zonal and meridional values, respectively.

The simulations performed here were essentially the classic single-particle dispersal problem, which consists of repeatedly dropping 1 particle into a fluid. Each release is considered independent, and Lagrangian statistics are compiled from an ensemble of many releases. In particular, a patch at time τ is the locations of all particles released from a particular location at time τ after their respective releases. The standard deviation of zonal displacement of a patch is (e.g. Davis 1991, Zhurbas & Oh 2003):

$$\sigma_x(\tau) = \langle x'(t_0 + \tau, t_0)^2 \rangle^{1/2} \quad (2)$$

where $x'(t,t_0)$ represents the zonal displacement (relative to the ensemble mean), at time t of a particle released at time t_0. The diffusivity is then estimated from the rate of change of the variance (SD squared)

$$K_x = \frac{1}{2} \frac{\partial \sigma_x{}^2}{\partial t} \quad (3)$$

Similar equations describe the meridional diffusivity, K_y.

Eq. (3) thus describes a method to calibrate the model: one can compute the displacement standard deviation from the GDP drifters that passed close to the islands, and do a similar calculation for the modelled larvae. If the model is calibrated properly, the resulting eddy diffusivities should be similar.

The model calibration simulations were made with 4 values of K^+: 0, 500, 1000 and 2000 m^2 s^{-1}. Because of computing restraints, the model calibration simulations were limited to 100 simulations (i.e. every 25 d for 6.5 yr).

Sixteen GDP drifters passed close to the islands. For each of these drifters, the displacement was computed relative to the mean trajectory of all the drifters that passed by its respective island. For example, the displacement for each drifter that passed by Campbell Island was computed by removing the mean trajectory of all 4 drifters that passed by that island. The numerical larvae were treated similarly, but in this case there are 400 drifters per ensemble (the 25 numerical drifters at each island are released at the same time in each simulation so they are not independent for the single-particle problem. Chatham Island releases were not used because these islands are too close to the edge of the domain. Thus, each of the other 4 islands contributes 1 numerical drifter for each of the 100 simulations.)

Zonal and meridional displacement variances for all model runs are plotted as a function of time in Fig. 4, together with the variance from the GDP drifters. Also plotted are the expected variances computed from Chiswell's (unpubl. data) estimates. Because of the different number of trajectories going into the ensemble means, one would expect the model values to be more stable than the GDP drifter values. In principle, one could compute expected error bars on these curves, but this was not done here because such errors are difficult to compute with any certainty, and as a practical matter, having error bars on the figure would not affect the choice of K^+.

Least-squares fits to the GDP variances provide eddy diffusivity estimates of 8×10^3 m^2 s^{-1} and 2.7×10^3 m^2 s^{-1} for the zonal and meridional directions, respectively, which are within the range of Chiswell's (unpubl. data) estimates.

Simulations made with no added diffusivity still show an overall diffusivity since each trajectory is different because releases are made over many months. For the zonal direction, simulations made with no added diffusivity show an overall diffusivity that is less than expected from the GDP drifters, but is consistent with Chiswell's (unpubl. data) lower estimates. Adding a random-walk raises the overall diffusivity, but there appears to be little sensitivity to the value of K^+. For the meridional direction, however, the runs made with no added diffusivity return an overall diffusivity that is well outside Chiswell's (unpubl. data) estimates, and adding a random-walk term results in overall diffusivity that is dependent on K^+, so that the best fit between GDP drifters and model occurs with $K^+ = 1000$ m^2 s^{-1}.

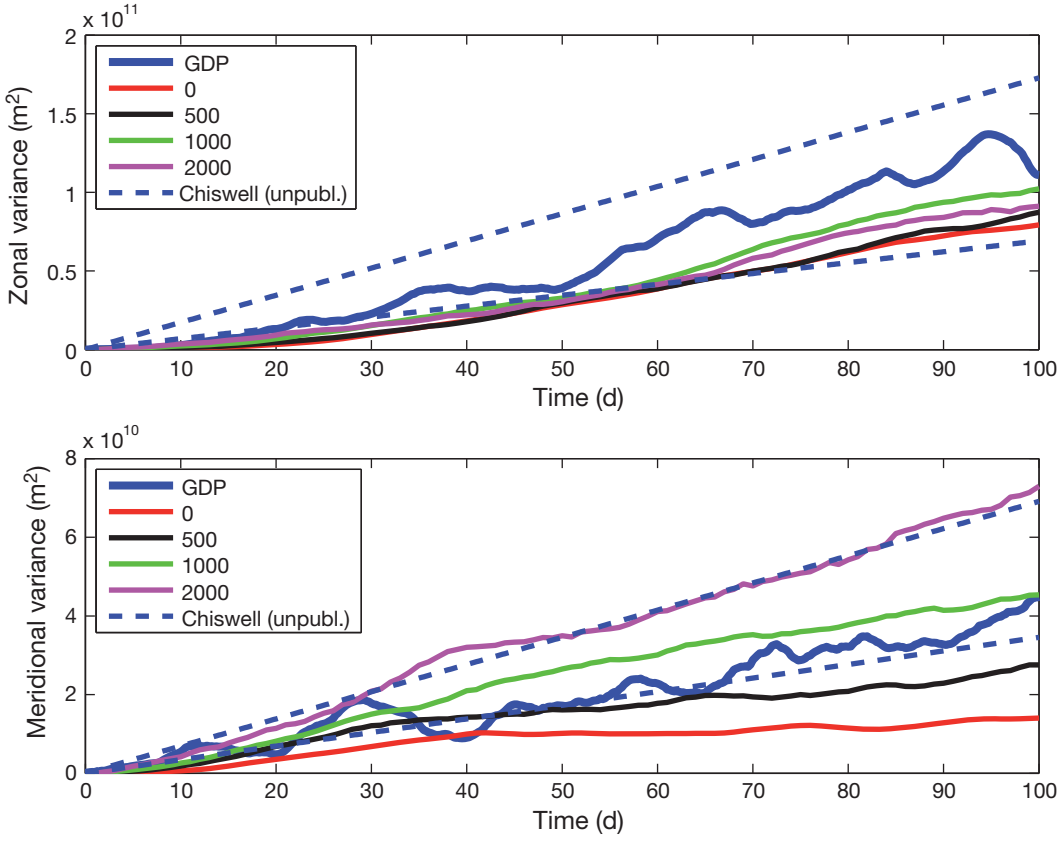

Fig. 4. Zonal and meridional displacement variances for model runs plotted as a function of time for K^+ = 500, 1000 and 2000 m^2 s^{-1} (see 'Model calibration'), together with the variance from the Global Drifter Program (GDP) drifters (thick lines). Also plotted are expected displacement variances (dashed blue lines) using Chiswell's (unpubl. data) estimates of overall eddy diffusivity

The level of anisotropy in overall diffusivity seen here (i.e. $K_x \sim 2K_y$) is fairly typical of temperate seas outside of western boundary currents (e.g. Zhurbas & Oh 2003), and is probably related to the fact that circulation is mostly zonal. However, it is not clear whether the added diffusivity, K^+, should also be anisotropic. The added diffusivity is designed to account for high-frequency mesoscale eddy variability that is not resolved in the AVISO currents, and there is no *a priori* reason to suggest that this mesoscale eddy variability is anisotropic. For this reason, and also since Fig. 4 suggests that overall diffusion in the zonal direction is relatively insensitive to the value of K^+, it was decided that the best overall value of diffusivity in the simulations would be obtained with setting the added diffusivity to be isotropic and have a value of $K^+ = 1000$ m^2 s^{-1}.

It should be noted that Eqs. (2) and (3) are often formulated in a tensor notation to consider the off-axes diffusivities (i.e. there is some correlation between the zonal and meridional random-walk terms, e.g. Zhurbas & Oh 2003), but this was not done here because adding such complexity was considered well beyond the limitations of the data available to validate such an approach. Thus, the zonal and meridional random-walk terms in this work were computed independently.

RESULTS

Seasonal and interannual trends

There could be seasonal and/or interannual fluctuations in the ocean currents around New Zealand that impact dispersal times. Larval spawning for many species is seasonal, and so it could be that dispersal times computed from all simulations, as done here, might be unrepresentative for certain species.

Fig. 5 shows the dispersal distance for a duration of 20 d (i.e. the distance larvae might travel from hatching to 20 d) for the Auckland Islands, plotted as a function of year-day, and as a function of time. While there is large short-term variability in the dispersal distance, there is little evidence of seasonality in the dispersal, and fits of a 365 d period annual cycle to the dispersal distance shown in Fig. 5 have no statistical significance (not shown). Similarly, there is little evidence of any interannual variability in the dispersal distances. Plots

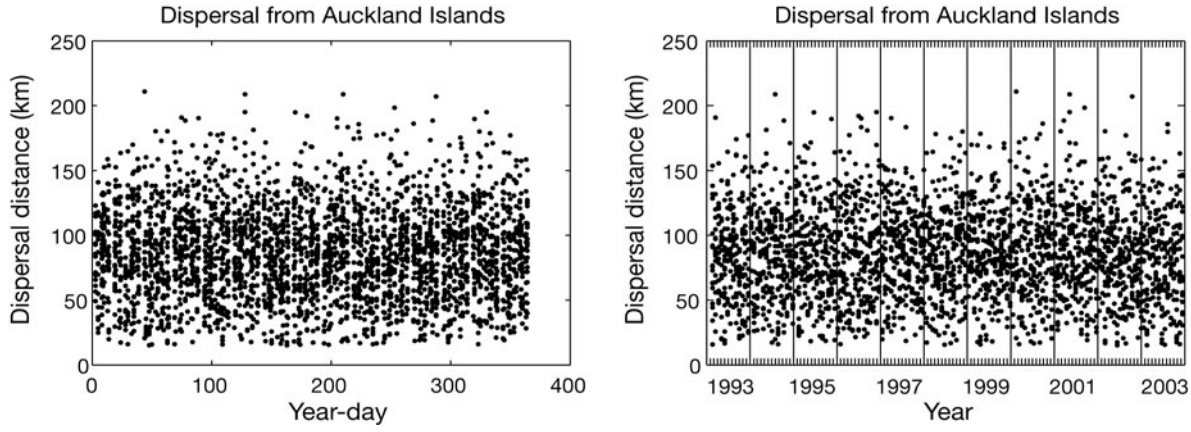

Fig. 5. Dispersal distance for 20 d (i.e. the distance larvae might travel from hatching to 20 d) for the Auckland Islands, plotted as a function of year-day (left panel) and as a function of time (right panel)

for the other islands and for other durations show similarly little temporal dependence of the dispersal distance.

Dispersal times

Simulations were made every 25 d from 1 January 1993 to 18 May 2007, thus there were 211 simulations in total. Each simulation was run for 300 d.

Simulated locations of larvae released around the main islands of New Zealand are shown for 5, 10, 20, 30, 50 and 100 d after hatching in Fig. 6. Each panel (A to F) also shows the locations of the GDP drifters that passed within 30 km of New Zealand at the corresponding time after closest approach. The locations of closest GDP drifter approach were not uniform around the country; 7 drifters were around the east coast of the North Island, 2 were from the south-west coast of the South Island, and the remainder were concentrated around the east coast of the South Island. There were 198 hatching locations around mainland New Zealand, so that if both modelled and GDP distributions accurately represent potential larval dispersal, the AVISO simulations and GDP locations could respectively be regarded as 41 778 (i.e. 198 × 211) and 21 samples of the true distribution. Given the high number of simulated larvae and low number of GDP drifters, one would expect the GDP drifter locations to be contained well within the envelope of the numerical simulations. This appears to be true for the 7 GDP drifters that originated near the North Island: for all dispersal times, the envelope of numerical simulations encompasses the North Island GDP drifters. However,

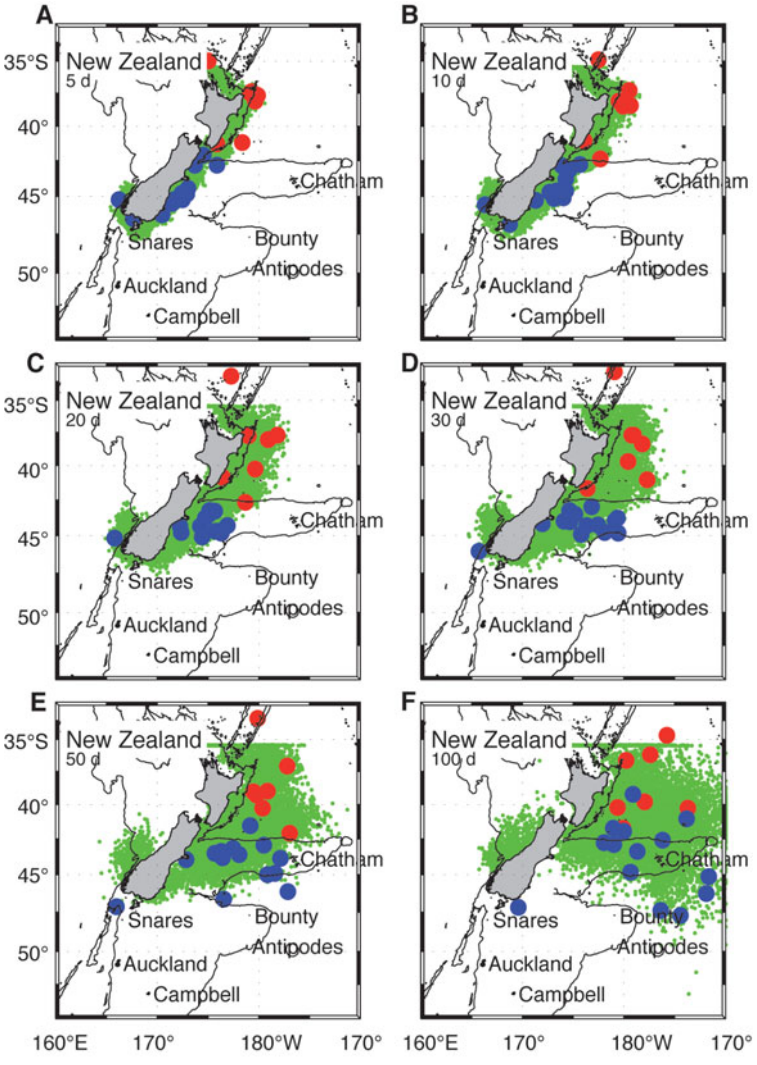

Fig. 6. Simulated larval locations after release from the main islands of New Zealand (green dots, see 'Dispersal times'). (A) 5; (B) 10; (C) 20; (D) 30; (E) 50; and (F) 100 d after release. Blue (red) dots show locations at the corresponding time since closest approach of Global Drifter Program drifters that passed within 30 km of the South (North) Island

it is not true for the drifters originating from the South Island. For example, some GDP drifters originating near the South Island extend beyond the cloud of numerical drifters. This suggests that the model may not capture the true variability of the currents off the east coast of the South Island.

Fig. 6 can be used to make qualitative estimates of the dispersal times between various islands. For example, the shortest travel time between New Zealand and the Chatham Islands appears to be somewhere between 30 and 50 d. The figure suggests that dispersal times from New Zealand to the Bounty Islands will be a little longer, and that that dispersal from New Zealand to either Auckland or Campbell Islands would occur at much longer timescales, if at all.

Figs. 7 to 11 show similar distributions of simulated larvae hatched at the offshore islands, together with the respective GDP drifters. There were 25 numerical releases at each island for each of the 211 simulations, giving a total of 5275 releases per island. Two GDP drifters passed within 30 km of the Auckland Islands, 4 passed within 30 km of Campbell Island, 4 passed within 30 km of the Antipodes Islands while 6 passed within 30 km of Bounty Island. No GDP drifters passed within 30 km of the Chatham Islands. Each panel also shows circles centred on the mean locations of the numerical and GDP drifters with a radius of 1 SD of the respective drifter displacements. The SDs computed for the GDP drifters are computed from few drifters, and may have little statistical significance.

The mean flow around the Auckland Islands is northwards, towards the South Island (Fig. 3), and both GDP drifters and numerical larvae travel in that direction (Fig. 7). While only 2 GDP drifters passed close to the Auckland Islands, there is remarkably good agreement between the numerical and GDP drifter locations

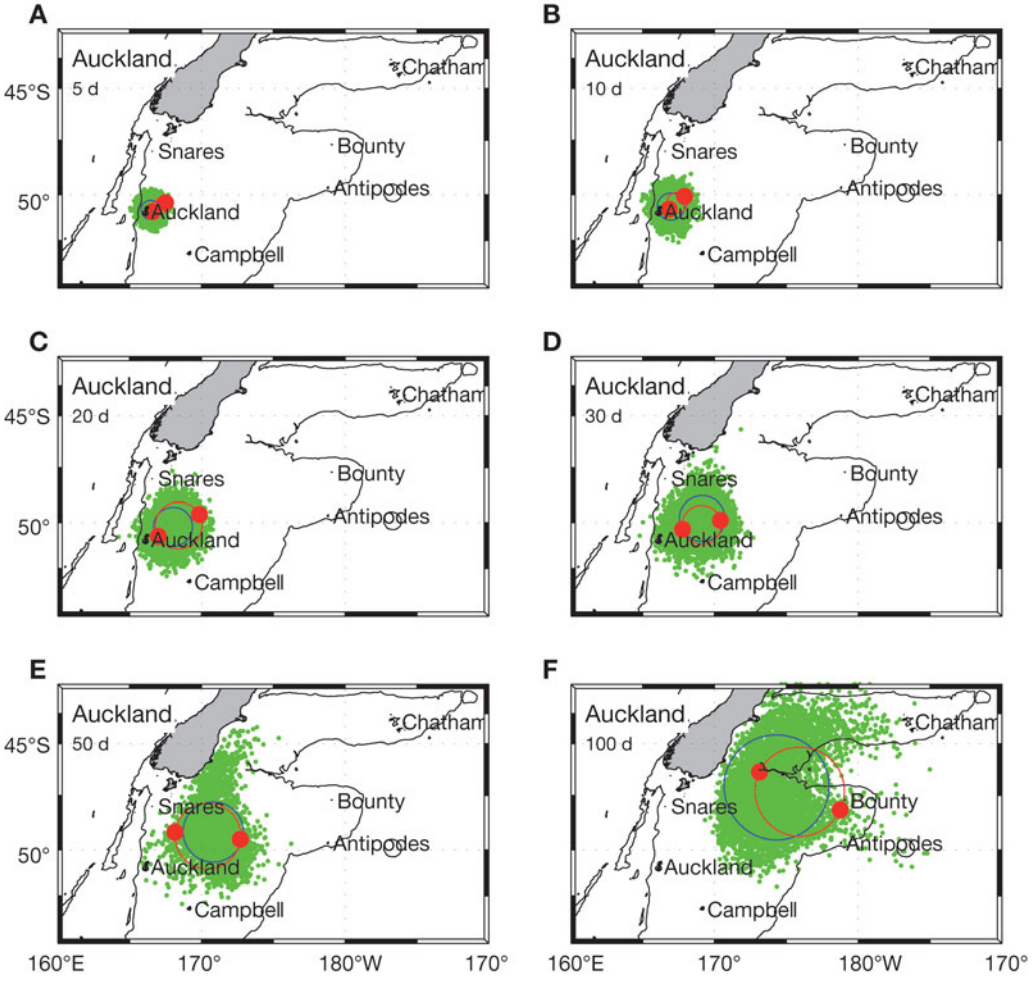

Fig. 7. Simulated larval locations for (A) 5; (B) 10; (C) 20; (D) 30; (E) 50 and (F) 100 d after release from Auckland Islands (green dots, see 'Dispersal times'). Red dots show locations at the corresponding time since closest approach of Global Drifter Program (GDP) drifters that passed within 30 km of Auckland Islands. Each panel also shows circles centred on the mean locations of the numerical and GDP drifters with a radius of 1 SD of the respective drifter displacements. Blue circles are for the numerical simulations, red circles are for the GDP drifters

as estimated by the standard deviations of the displacements. The figure suggests that minimum dispersal times from the Auckland Islands are likely to be between 30 and 50 d to mainland New Zealand, and 50 to 100 d to Bounty or the Chatham Islands.

The mean flow around Campbell Island is approximately north-east, and Fig. 8 shows that both GDP drifters and numerical larvae travel towards Bounty and Antipodes Islands. The GDP drifters tend to travel a little faster than the numerical larvae, and the figure suggests that minimum dispersal times from Campbell Island are likely to be about 30 d to the Antipodes Islands, 50 d to Bounty Island and over 100 d to the Chatham Islands. It appears that Campbell Island is upstream from both the Auckland Islands and mainland New Zealand, so that larvae are unlikely to disperse from Campbell Island to either the Auckland Islands or mainland New Zealand.

The mean flow near Bounty and Antipodes Islands is to the east, and Figs. 9 & 10 show that both GDP drifters and numerical larvae from these islands disperse to the east. The GDP drifters that passed close to the Antipodes Islands tend to travel eastwards faster than numerical larvae released near the islands, but there is much better agreement between the drifters and numerical simulations for Bounty Island releases. The figure suggests that dispersal from Antipodes Islands to Bounty Island could be as low as 10 d, whereas dispersal times in the opposite direction are likely to be much longer. Minimum dispersal times from either of these islands to the Chatham Islands could be as short as about 30 d.

The Chatham Islands sit in relatively strong eastward flow at the eastern end of the Chatham Rise, and the simulations (Fig. 11) indicate that there may be some dispersal to the south so that minimum dispersal times to the Bounty Islands could be about 30 to 50 d, but other than this connection, it seems unlikely that larvae from the Chatham Islands would reach any of the other islands.

Quantitative estimates of dispersal time can be made by compiling histograms of the simulated dispersal

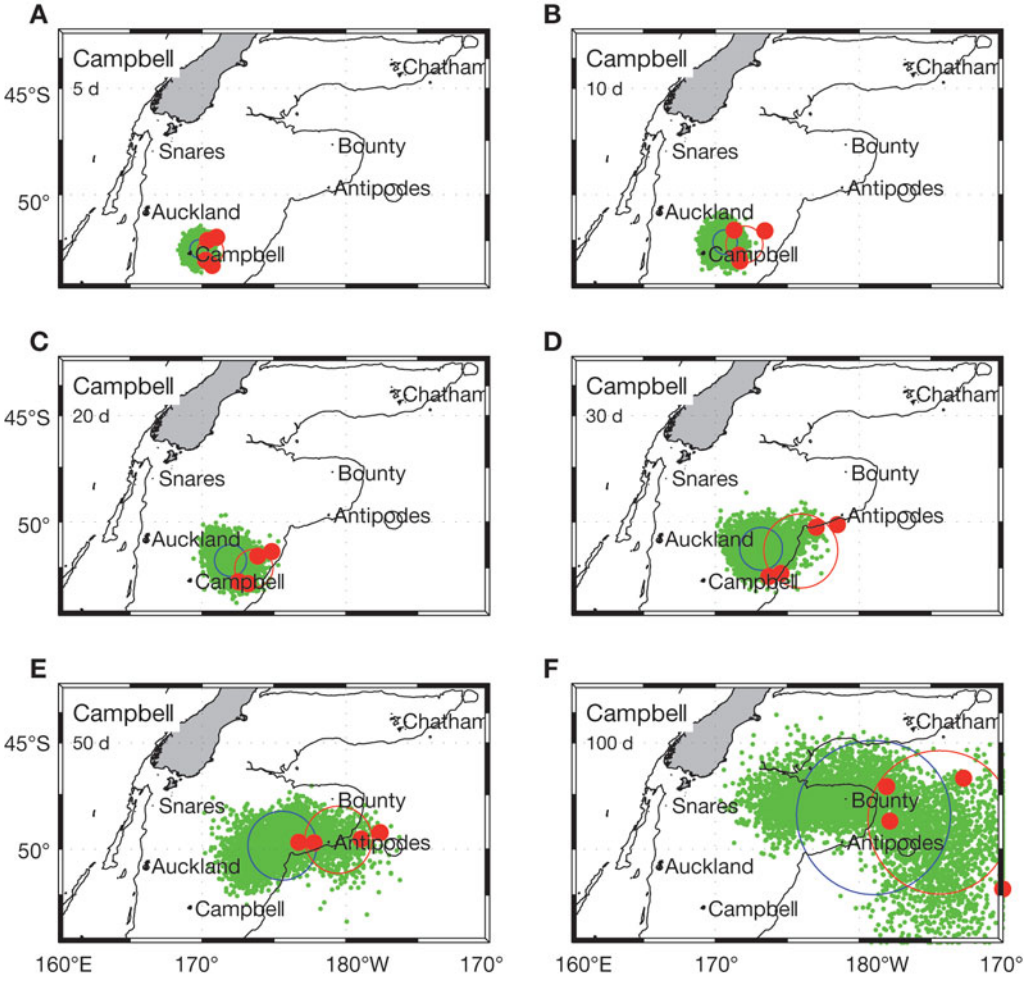

Fig. 8. Simulated larval locations. As in Fig. 7, but for releases from Campbell Island

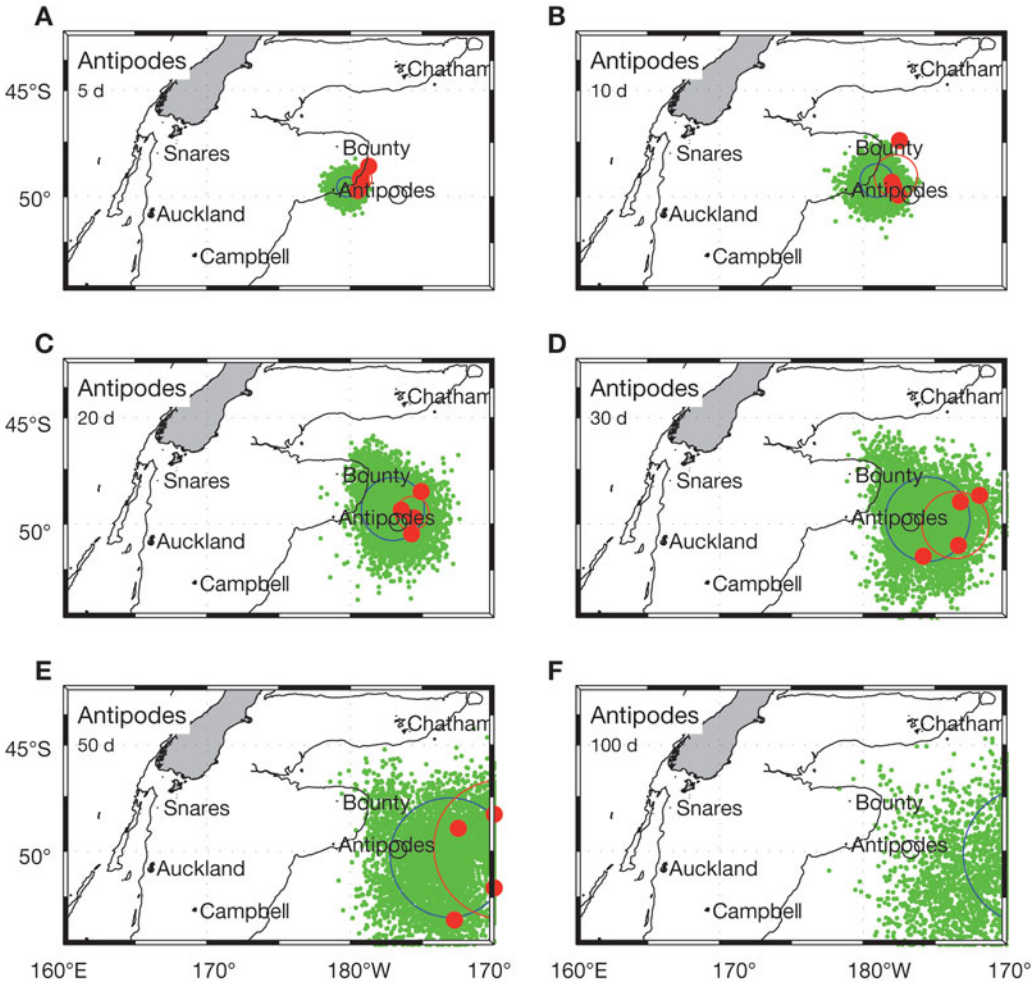

Fig. 9. Simulated larval locations. As in Fig. 7, but for releases from the Antipodes Islands

times between source and destination islands. Few numerical larvae pass exactly through the destination islands, so numerical drifters are considered to have arrived at an island if they pass through a circle defined by 1 'arrival radius' from the island. This radius should be chosen so that the statistics of all arrival times within the arrival circle are the same. Here the arrival radius was chosen to be 50 km so that the arrival circles approximate the size of the Chatham Islands (this radius is shown in Fig. 3).

Fig. 12 shows histograms for all island pairs where arrivals were recorded. When the destination island is directly downstream from the source island, as many as 12% of released larvae arrive. The best resolved histogram of dispersal time is for New Zealand to the Chatham Islands, where 4049 arrivals were recorded. The mean dispersal time was 125 d, but the distribution is positively skewed so that the median dispersal time is 111 d, and the minimum dispersal time was 46 d. When the arrival island is not directly downstream, far fewer arrivals occur. Just 5 larvae released from mainland New Zealand arrived at Bounty Island. Thus, the histograms necessarily have low resolution for many island pairs.

Because of the large range in the number of arrivals, one cannot directly compare the minimum simulated dispersal times for different island pairs — the shortest simulated dispersal times for Campbell to Antipodes and Bounty to Chatham Islands were both 35 d, but the former island pair had 1243 arrivals compared to 32 for the latter. In addition, the shortest dispersal time computed from 15 yr of simulations is unlikely to represent the minimum dispersal time had the simulations been run for significantly longer. One way around these issues is to fit an analytic function to the histograms, and specify a percentile dispersal time from the fits to be a proxy for the minimum dispersal time. The problem then becomes one of deciding which percentile to choose, and this will depend on the problem of interest. For example, if genetic connectivity requires less gene flow than ecological connectivity, one would choose a lower percentile value for genetic connections than for ecological connections.

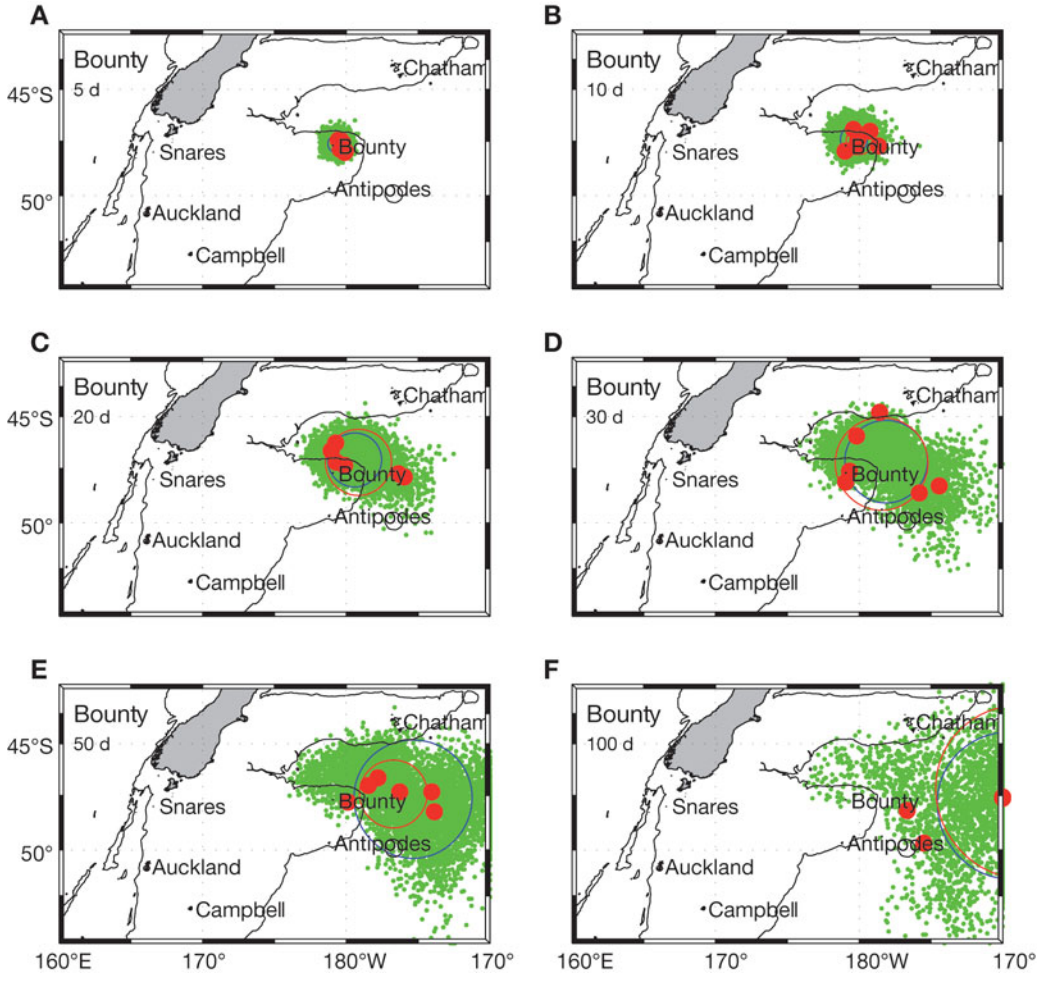

Fig. 10. Simulated larval locations. As in Fig. 7, but for releases from Bounty Island

Each of the relatively well resolved histograms is positively skewed and appears approximately log-normal. Thus log-normal fits were made to each distribution as shown in Fig. 12. Once these fits were made, various percentile values were computed, and the figure also shows the 1, 10^{-2} and 10^{-4} percentile dispersal times derived from the fits. These represent the 1 in 100, 1 in 10 000 and 1 in 1 million ranked arrival times (i.e. from the left side of the distributions), and are designated as T_{100}, T_{10000} and T_{1e6}, respectively.

One and 10^{-4} percentile dispersal times derived from the log-normal fits are shown in Table 1 for all island pairs. The smallest 1 percentile value, T_{100}, between any of the islands is 10 d (Antipodes to Bounty Island), but all other values of T_{100} are longer than 10 d. Thus, if one takes 10 d to be the maximum larval duration for *Cellana* spp. (Creese 1981), the T_{100} dispersal times are too long to explain the observed genetics. This is also true of T_{10000}, and one needs to choose a value at least as low as the 10^{-4} percentile, T_{1e6}, to begin to explain the genetics. With T_{1e6} as the proxy, in the western lineage one obtains gene flow between the Auckland Islands and both New Zealand (T_{1e6} = 11 d) and Campbell Island (T_{1e6} = 10 d). In the eastern lineage, gene flow can occur between Antipodes and Bounty, but not between Bounty and Chatham Islands (although this island pair is poorly resolved). The shortest value of T_{1e6} between the lineages is 26 d between Campbell and Antipodes Islands, which is long enough to separate the lineages. If one chooses T_{1e9} (not listed) instead of T_{1e6}, dispersal times decrease so that all connections within each lineage appear; there would be gene flow between Campbell Island and mainland New Zealand in the western lineage, and in the eastern lineage, the Chatham Islands would become connected to Bounty Island.

DISCUSSION

The main finding to be derived from this work for *Cellana strigilis* is that some islands are genetically

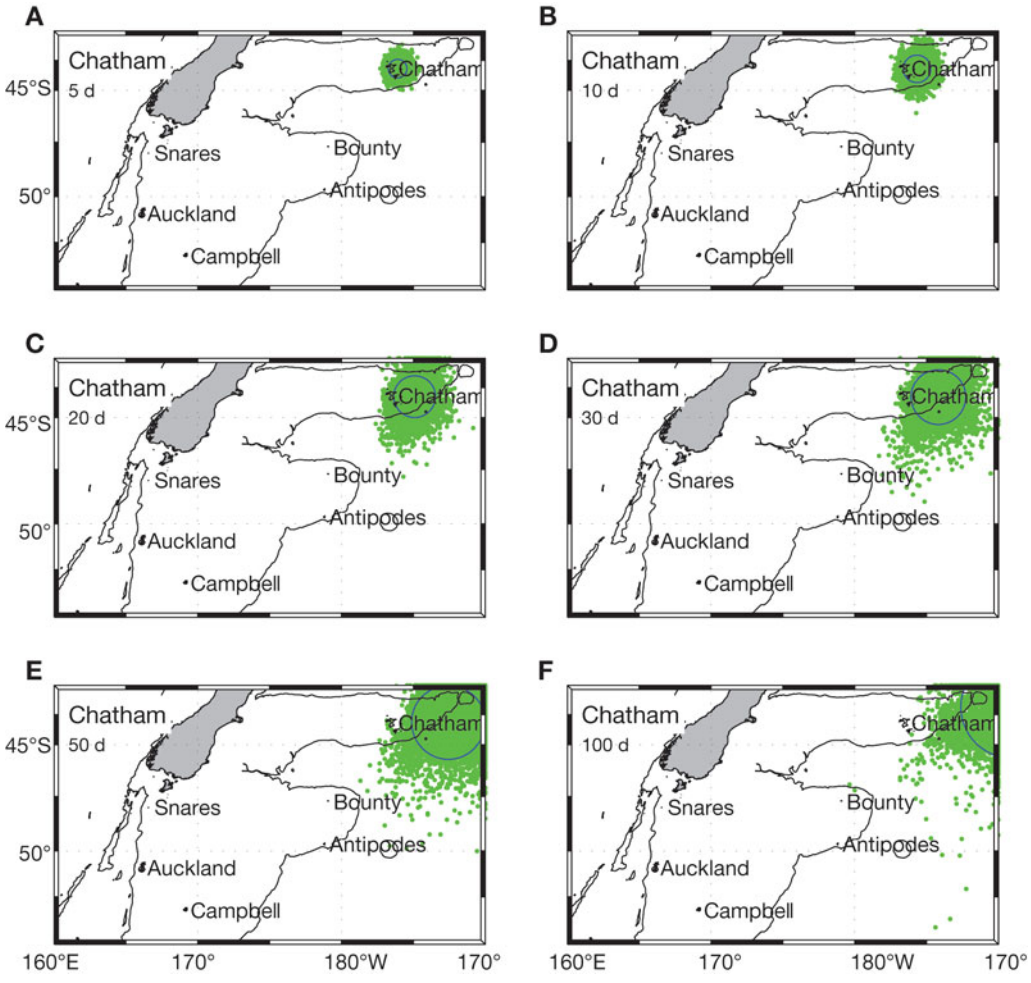

Fig. 11. Simulated larval locations. As in Fig. 7, but for releases from the Chatham Islands

connected even when they are so far apart that the minimum simulated dispersal time between them is much longer than the maximum larval duration. It is only between Antipodes and Bounty Islands that simulated dispersal times approach the larval duration. If the present-day genetic structure for the other genetically connected island pairs is being maintained by larval dispersal, then it is being maintained by events that

Table 1. One and 10^{-4} percentile dispersal times (days) between New Zealand and SubAntarctic Islands. One (T_{100}) and 10^{-4} (T_{1e6}) percentile dispersal times derived from log-normal fits to the histograms of dispersal times (see text and Fig. 12). The table should be read as rows only. For example, the 1 and 10^{-4} percentile dispersal time from the main islands of New Zealand to the Chatham Island are 56 and 27 d, respectively. >>: no arrivals occurred in the simulations. Values for Antipodes to Chatham Islands and Bounty to Antipodes Islands are listed as a range and a question mark to indicate that no arrivals were simulated, but estimates were made from the distributions of simulated larvae (Figs. 9 & 10)

T_{100}, T_{1e6}	Destination					
	To mainland NZ	To Auckland	To Campbell	To Antipodes	To Bounty	To Chatham
From mainland NZ	–	>>	>>	>>	64, 31[a]	56, 27
From Auckland	32, 11	–	20,10[a]	69, 40	94, 55	117, 72
From Campbell	50, 18[a]	>>	–	36, 20	57, 30	123, 80
From Antipodes	>>	>>	>>	–	10, 4[a]	50–100?
From Bounty	>>	>>	>>	30–50?	–	35, 15
From Chatham	>>	>>	>>	>>	>>	–

[a]A fit is made to a histogram with few arrivals

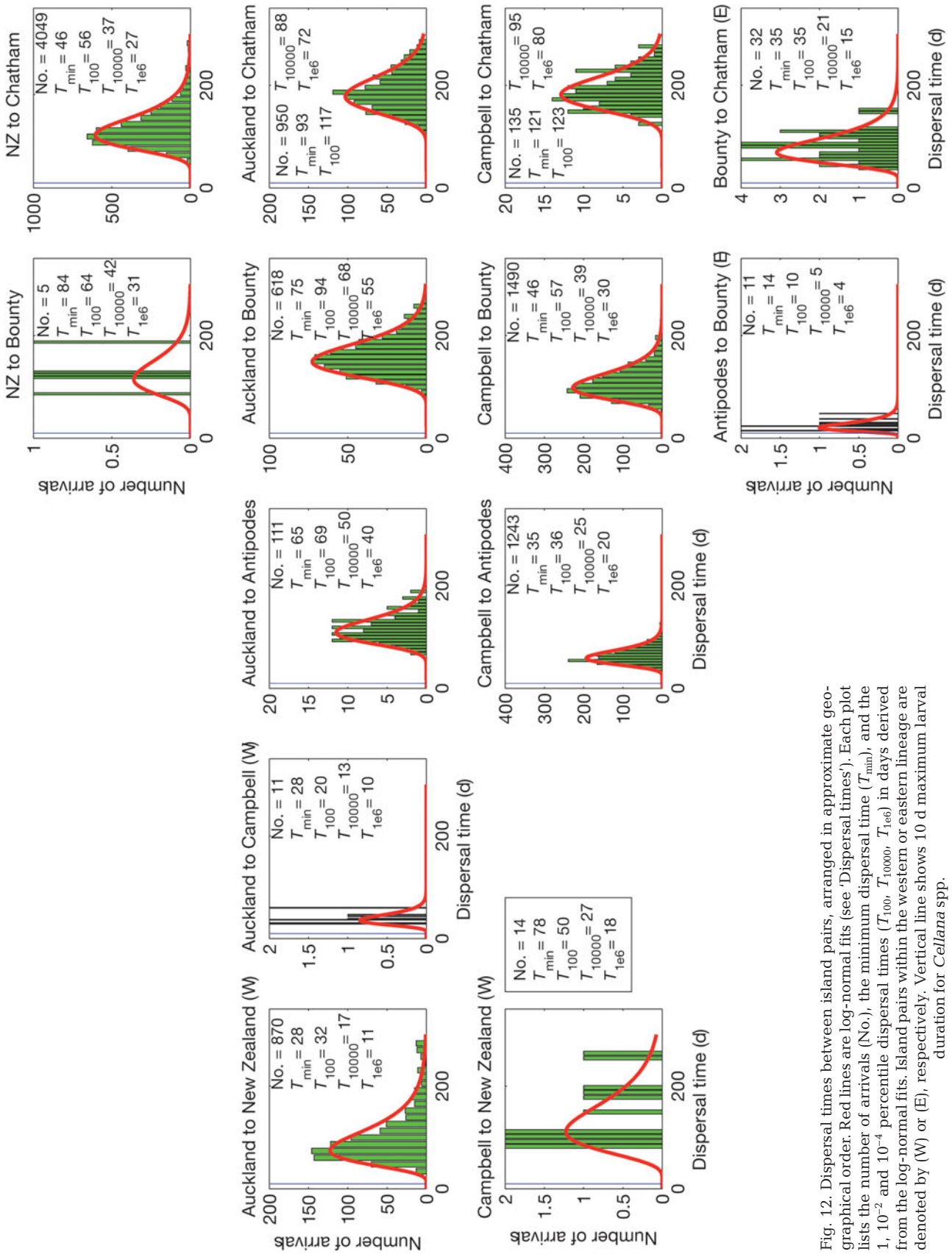

Fig. 12. Dispersal times between island pairs, arranged in approximate geographical order. Red lines are log-normal fits (see 'Dispersal times'). Each plot lists the number of arrivals (No.), the minimum dispersal time (T_{min}), and the 1, 10^{-2} and 10^{-4} percentile dispersal times (T_{100}, T_{10000}, T_{1e6}) in days derived from the log-normal fits. Island pairs within the western or eastern lineage are denoted by (W) or (E), respectively. Vertical line shows 10 d maximum larval duration for *Cellana* spp.

occur too infrequently to be modelled directly. It appears that very infrequent connection is sufficient to maintain genetic homogeneity.

This work illustrates 2 common problems with using models to estimate connectivity. The first is that models often (perhaps usually, e.g. Cowen et al. 2003) miss some of the relatively high frequency eddy variability. It is possible to add a random walk term to compensate for this missing variability, and here, GDP drifter data were used to calibrate the model so that the overall eddy diffusivity in the simulations approximately matches that seen in the drifter data. This model calibration is not unambiguous, partly because there are few drifters in the region, and partly because parameterising missing dispersal in terms of a single eddy diffusivity coefficient may be simplistic (Rupolo 2007).

The second, and perhaps bigger, problem is in accumulating enough arrivals to estimate the statistics of the dispersal times. Where the destination island is downstream of the source island, it is reasonably quick to accumulate enough arrivals to build a histogram. By making some assumptions about the distribution of the histogram (in this work, log-normal), it is possible to compute various percentile arrival times from the analytical fit. However, when the destination island is not directly downstream of the source island, it can be virtually impossible to get enough arrivals to compute the histogram, as in the Auckland to Campbell Islands, where there were only 11 arrivals. In some cases, there were no arrivals, even though the simulated distributions skirt the destination island; for example, a visual analysis of the Antipodes to Chatham Islands simulations seen in Fig. 9 would suggest that arrival times at the Chatham Islands could be as low as 50 d. Yet no larvae in the simulations arrived within 50 km of the Chatham Islands, even after 300 d. One can improve the number of arrivals slightly by increasing the arrival radius, but there is a limit to which this arrival radius can be increased. To obtain enough arrivals to compute the histogram would require many more simulations (perhaps several orders of magnitude) than made here, and so becomes computationally infeasible.

Even if histograms are well computed, there is still the problem of determining whether any percentile arrival time can be taken as a proxy for rare events. There are 2 issues here: (1) whether the AVISO currents (plus added diffusivity) accurately simulate all processes leading to the rare events — in other words, are the rare events just extremely unlikely cases of mesoscale variability combining to produce fast transits, or are they caused by physical processes that are not modelled by AVISO currents? It may be, for example, that long-distance dispersal is due to extreme wind-forcing that does not lead to a sea surface expression, and so would not appear in the AVISO currents. Or it may be that some biological process, such as rafting, aids in the dispersal. (2) Whether one can accurately compute percentile values that are so far down the distributions from the analytic fits, even if the AVISO currents simulate all the variability. It may be that the true distributions are sufficiently non log-normal that the tails are poorly calculated.

None of these issues can be resolved from modelling studies, but if the T_{1e6} values are indicative of the true infrequency at which gene flow can occur, then one would need an order of 1×10^6 simulated arrivals to observe 1 arrival that is less than a *Cellana* larval lifetime. This would require about 250 times the simulations made here for Auckland Islands to New Zealand, and 100 000 times the simulations made here for Auckland to Campbell Islands. Even if the percentile estimates are wrong by an order of magnitude, it would appear that one cannot run enough simulations to fully describe rare-event statistics.

In reality, gene flow is determined by the total number of larvae arriving at any island, and this depends on larval mortality as well as the dispersal times. Dispersal statistics can be used (Fig. 12) to estimate the long-term probability that an individual larva travels between islands. For example, since New Zealand is a relatively large target, approximately 16% of the simulated larvae released at the Auckland Islands arrive in New Zealand, although only 1 in 1 million dispersal times is less than the 10 d maximum larval duration of *Cellana* spp. Larval mortality rates from hatching to settlement are notoriously variable; for example, Cowen et al. (2000) commented that published estimates of larval mortality rates range from 0.03 to 0.62 d^{-1} (i.e. survival rates from 0.73 to 6×10^{-5} over 10 d), and they used a mode value of 0.2 d^{-1} (survival rate of 0.1 over 10 d) in their modelling. Taking their mode value and our dispersal time statistics, one obtains the chance of an individual *Cellana* larva released at the Auckland Islands and settling in New Zealand to be about 2×10^{-8}, although given the uncertainties in the model and in mortality rates, this estimate has to be regarded as having huge uncertainty. For larval transport from Antipodes to Bounty Island, the target is smaller (0.2% of simulated larvae arrive), but the larval duration falls at the 1 percentile value, so that taking the same mortality (0.2 d^{-1}) leads to the chance of an individual larva from the Antipode Islands settling in Bounty Island to be about 2×10^{-6}. One might make the observation that a settled larva only contributes to the gene pool only if it grows to maturity, and its offspring also settle, so there is an additional level of mortality that needs to be considered when computing the gene flow.

Thus, the main conclusions drawn from this work are that genetic connectivity appears within island pairs even where the combination of rare dispersal, low target size and mortality leads to nearly vanishingly small chances for individual larvae to settle. If genetic connectivity occurs between these islands due to larval dispersal, it is only because benthic invertebrates are either so numerous and/or so fecund and/or that it only requires a very small amount of gene flow between populations to maintain genetic homogeneity that they overcome these extremely low probabilities of success for individual larvae.

Overall, as might be expected, larval dispersal reflects the mean circulation. Larvae hatched around the main islands of New Zealand end up east of the country, and so, for example, it is easier for larvae hatched off the South Island to drift to the Chatham and Bounty Islands than for them to drift to the Auckland Islands. Similarly, larvae hatched off either the Auckland or Campbell Islands are more likely to drift to the Bounty or the Antipodes Islands than between each other. Bounty and the Antipodes Islands are close enough together in a region of relatively weak mean flow that dispersal between them is largely controlled by mesoscale eddy variability. The Chatham Islands are so far downstream that significant larval dispersal between them and the other Sub-Antarctic islands is unlikely.

Acknowledgements. Thanks to S. Goldstien for suggesting this as an interesting topic and 2 anonymous reviewers for their constructive comments. This work was funded by the Foundation for Research, Science and Technology, New Zealand, Contract No. C01X0223.

LITERATURE CITED

Booth JD (2002) Early life history, recruitment processes and settlement of spiny lobsters. Fish Sci 68:384–389

Chiswell SM, Rickard GJ (2006) Comparison of model and observational ocean circulation climatologies for the New Zealand Region. J Geophys Res 111 doi:10.1029/2006JC003489

Chiswell SM, Rickard GJ (2008) Eulerian and Lagrangian statistics in the Bluelink numerical model and AVISO altimetry: validation of model eddy kinetics. J Geophys Res 113:C10024 doi:10010.11029/12007JC004673

Chiswell SM, Rickard GJ, Bowen MM (2007) Eulerian and Lagrangian eddy statistics of the Tasman Sea and southwest Pacific Ocean. J Geophys Res 112 doi:10.1029/2007JC004110

Cowen RK, Sponaugle S (2009) Larval dispersal and marine population connectivity. Annu Rev Mar Sci 1:443–466

Cowen RK, Lwiza KM, Sponaugle S, Paris CB, Olson DB (2000) Connectivity of marine populations: open or closed? Science 287:857–859

Cowen RK, Paris CB, Olson DB, Fortuna JL (2003) The role of long distance dispersal in replenishing marine populations. Gulf Caribb Res 14:129–137

Creese RG (1981) Patterns of growth, longevity and recruitment of intertidal limpets in New South Wales. J Exp Mar Biol Ecol 51:145–171

Davis R (1991) Observing the general circulation with floats. Deep-Sea Res I 38:S531–S571

Futuyma DJ (1998) Evolutionary biology, Edn 3. Sinauer, Sunderland, MA

Goldstien SJ, Schiel DR, Gemmell NJ (2009) Colonisation and connectivity by intertidal limpets among New Zealand, Chatham and SubAntarctic Islands. I. Genetic connections. Mar Ecol Prog Ser 388:111–119

Hansen DV, Poulain PM (1996) Quality control and interploations of WOCE/TOGA drifter data. J Atmos Ocean Technol 13:900–909

Kinlan BP, Gaines SD, Lester SE (2005) Propagule dispersal and the scales of marine community process. Divers Distrib 11:139–148

Mace GM, Lande R (1991) Assessing extinction threats: toward a reevaluation of IUCN threatened species categories. Conserv Biol 5:148–157

Mills LS, Allendorf FW (1966) The one-migrant-per-generation rule in conservation and management. Conserv Biol 10:1509–1518

Niiler PP, Sybrandy AS, Bi K, Poulain PM, Bitterman D (1995) Measurements of the water-following capability of holey-sock and TRISTAR drifters. Deep-Sea Res I 42: 1951–1964

Olson DB (2007) Lagrangian biophysical dynamics. In: Griffa A, Kirwin AD, Mariano AJ, Özgökmen T, Rossby HT (eds) Lagrangian analysis and prediction of coastal and ocean dynamics. Cambridge University Press, Cambridge, p 275–348

Pond S, Pickard GL (1978) Introductory dynamical oceanography, Pergamon, Oxford

Rupolo V (2007) Observing turbulence regimes and Lagrangian dispersal properties in the oceans. In: Griffa A, Kirwin AD, Mariano AJ, Özgökmen T, Rossby HT (eds) Lagrangian analysis and prediction of coastal and ocean dynamics. Cambridge University Press, Cambridge

Stephens SA, Broekhuizen N, Macdiarmid AB, Lundquist CJ, McLeod L, Haskew R (2006) Modelling transport of larval New Zealand abalone (*Haliotis iris*) along an open coast. Mar Freshw Res 57:519–532

Walker MM (1984) Larval life span, larval settlement, and early growth of *Evechinus chloroticus* (Valenciennes). N Z J Mar Freshw Res 18:393–397

Zhurbas V, Oh IS (2003) Lateral diffusivity and Lagrangian scales in the Pacific Ocean as derived from drifter data. J Geophys Res 108:3141 doi:3110.1029/2002JC001596

Editorial responsibility: Antony Underwood, Sydney, Australia

Submitted: September 30, 2008; Accepted: June 18, 2009
Proofs received from author(s): July 24, 2009